

A mechanics based prediction model for tool wear and power consumption in drilling operations and its applications

Qi Wang^a, Dinghua Zhang^{a, **}, Kai Tang^{b, *}, Ying Zhang^a

^a The Key Laboratory of Contemporary Design and Integrated Manufacturing Technology, Ministry of Education, Northwestern Polytechnical University, China

^b The Hong Kong University of Science and Technology, Hong Kong

ARTICLE INFO

Article history:

Received 11 March 2019
Received in revised form
14 May 2019
Accepted 13 June 2019
Available online 20 June 2019

Handling Editor: Baoshan Huang

Keywords:

Energy consumption modelling
Drilling
Cutting force
Tool wear
Parameter optimization

ABSTRACT

We present a mechanics based model for predicting the power consumption of drilling operations. Different from existing power models in machining that ignore the tool wear, our model takes into full consideration the tool wear which is particularly pronounced in drilling and causes extra power consumption. For any given spindle speed n and feed rate f , our model establishes the relationship between the length of drill and the total power consumption as well as the amount of tool wear. With this prediction model established, we can then optimize the drilling parameters (n, f) towards different objectives, such as the two applications reported in this paper – to minimize the average power consumption per unit length of drill and to maximize the tool usage before its replacement. Physical drilling experiments of the proposed power prediction model and its two optimization applications are also reported in this paper which have validated the accuracy of the model and convincingly demonstrated its efficacy in deciding optimal drilling parameters (n, f) for energy minimization and other objectives.

© 2019 Elsevier Ltd. All rights reserved.

1. Introduction

Drilling is a simple yet fundamental machining operation needed in many manufacturing applications. For example, it is estimated that there are more than 6500 holes in a medium-sized aeroplane (Portillo et al., 2012) and most of them are drilled. When drilling on hard materials (such as Nickel-based super-alloy) which are commonly used for aeronautical parts, the biggest concern is the wear of the tool as it typically deteriorates very fast due to the exceedingly large cutting force (Sun et al., 2015). As drilling is simple, when the tool is fixed, the only affecting machining parameters are the spindle rpm n and tool feed rate f . The fundamental process planning task is then to determine a best pair of (n, f) towards various objectives. In particular, amid today's high societal attention on sustainability, the following objective on energy minimization naturally rises: how to plan (n, f) to minimize the average power consumption per unit length of drill? Another objective that is related to the cost of tool could be: given a tool

replacement threshold on the tool wear (i.e., the maximum tool wear at which the tool must be replaced), how to find the best (n, f) so that the maximum length of drill can be achieved by a single tool? A similar minimization problem could also be defined on time efficiency. These objectives are different and may conflict each other. Regardless, the fundamental prerequisite is a correct modelling of the relationship among the tool wear, the length of drill, the power consumption, and the machining parameters (n, f) .

Particularly pertinent to the subject of energy minimization in machining, numerous energy consumption models have been reported in the past decade. For example, Gutowski et al. (2009) is the first who put forward the theory that energy consumption is linearly related to the material removal rate (MRR) in a typical machining process. Kara and Li (2011) proposed a model of specific energy consumption (SEC), which is associated with the MRR and can be applied to both lathes and milling machines. These models however only consider MRR and thus are inaccurate when other factors (such as spindle speed) become critical. Subsequently, Li et al. (2013) proposed an energy model which is based on thermal equilibrium and considers the spindle speed in air-cutting. The prediction accuracy of the model is found to be significantly improved compared to the first two models. Recently Zhong et al. (2017) proposed the so called decision rules on deciding the

* Corresponding authors.

** Corresponding author.

E-mail addresses: dhzhang@nwpu.edu.cn (D. Zhang), mektang@ust.hk (K. Tang).

Nomenclature			
<i>abbreviations</i>			
MRR	material removal rate	θ	angle between the x -axis and the cutting velocity
SEC	specific energy consumption	γ_d	angle between the tapered cutting edge and the component of the cutting speed in the y direction
<i>symbols</i>		i	angle between the cutting velocity and the normal to the cutting edge
dF_t, dF_f, dF_r	components of differential cutting force in tangential, feed and radial direction	K_{zc}, K_{ze}	specific cutting force and edge force coefficient
K_{tc}, K_{fc}, K_{rc}	specific cutting force coefficients	F_{zw}, F_{tw}	additional forces in both the axial direction and the cutting direction
K_{te}, K_{fe}, K_{re}	specific edge force coefficients	σ	stress of the rebound frictional contact surface
dA	area of the differential chip lip being removed	E	modulus of elasticity
h	chip thickness	δ	material rebound rate
c	feed rate [mm/r]	μ	sliding friction coefficient
f	feed rate [mm/min]	$\Delta K_{rw}, \Delta K_{zw}$	tool wear coefficients
n	spindle speed	$P_{rotation}$	total power consumed due to the rotational motion
$V(z)$	cutting velocity	P_{feed}	total power consumed due to the feed motion
κ_t	taper angle	$P_{cutting}^w$	cutting power considering tool wear
Δb	chip width	P_{idle}	idle power
dz	chip height	$P_{cutting}$	cutting power
		$P_{auxiliary}$	auxiliary power
		P_{total}	total power
		L	length of drill

minimum energy consumption in turning, which take into account the effects of different cutting parameters on MRR. However, different cutting parameters may result in a same MRR. This is especially the case in drilling, as the MRR in drilling depends on only the feed rate but independent of the spindle speed, while numerous drilling experiments have shown that the power consumption in drilling is significantly influenced by the spindle speed. Different from the MRR based models, Li and Kara (2011) presented an energy consumption model for machining that is based solely on the cutting force. Later, Liu et al. (2015) proposed a hybrid approach for modelling the energy consumption in milling processes, which according to their experiments is able to achieve a relatively high accuracy. In their model, the cutting power is calculated based on the cutting force, while empirical calibrations are used to calculate the total power. Also based on the cutting force, Xu et al. (2016) proposed a tool path generation algorithm for minimizing the total energy consumption of five-axis milling of freeform surfaces. More recently, Watson and Taminger (2018) proposed a model that considers the entire manufacturing lifecycle – from the production and transport of feedstock material through processing to return of post-production of scrap for recycling. Jia et al. (2018) established a novel energy model of machine-operator systems to assess the energy efficiency of machining processes, which achieved a near 16% saving in energy consumption in their test case of verification. Wang et al. (2018) presented a cutting energy consumption model for prismatic machining features (PMFs), which according to their tests achieved good prediction results. Zhao et al. (2019) studied the impact of surface machining complexity (SMC) on energy consumption and efficiency in CNC machining and proposed a processing method to save the energy and improve the machining efficiency. Camposeco-Negrete et al (2019) proposed a method to optimize the machining parameters of AISI 1045 steel for turning to reduce the energy consumption and surface roughness. Zeng et al. (2019) experimentally fitted a specific energy consumption (SEC) model and claimed an over 90% prediction accuracy.

Nonetheless, all the above models ignore the impact of tool wear on energy consumption, while tool wear is inevitable in actual machining, and particularly serious in drilling operations. Previous

studies have shown that tool wear during machining often significantly changes the cutting force. In terms of the related studies, Iliescu et al. (2010) established a drilling thrust force model considering the tool wear and investigated the relationship between the machining parameters and tool wear. Sun et al. (2013) pointed out that as the tool wear aggravates, the cutting force will increase significantly. Hou et al. (2015) showed that tool wear can induce additional frictional and squeezing forces in the cutting area. Fernández-Pérez et al. (2017) investigated how to detect tool wear in drilling and select better machining parameters to extend the tool life. Luo et al. (2018) also studied the effect of tool wear on tool life in five-axis milling and proposed a strategy of averaging out the tool wear on the cutter so to extend the tool life. Obviously, as the cutting force is increased by the tool wear, so will be the energy consumption. Earlier studies have already found that the cutting energy is closely related to the tool's state, and the cutting power is linear with the tool wear (Cuppini et al., 1990). Shao et al. (2004) considered the effect of average tool wear on the cutting power and proposed a corresponding milling energy consumption model. Yoon et al. (2013, 2014) also considered the tool wear in their energy consumption model of milling machines, and they found that the material removal rate often increases as the tool wear worsens. Liu et al. (2016) studied the effects of tool wear on energy consumption and established an energy model. Recently, Shi et al. (2018) established a milling power consumption model based on the cutting force, which considers the effect of tool wear. Proteau et al. (2019) used the power signal calculated from the MRR to predict the tool wear through a neural network algorithm with a prediction accuracy of over 90% in their tests. Wang et al. (2019) employed a data dependent system (DDS) to study the energy consumption and tool wear of spindle motors during hard milling. Tian et al. (2019) proposed a process parameter optimization method that takes into account the tool wear to reduce the carbon emissions during machining.

Unfortunately, the aforementioned models, though having considered the tool wear in different degrees, are applicable only to milling operations which cannot be used for drilling operations. More explicitly, there has not been any published study on how to

establish a prediction model for drilling that is able to correctly define the relationship among the tool wear, the length of drill, the power consumption, and the machining parameters (n, f), and this is exactly the objective of this paper.

Specifically, in this paper, we will present a drilling energy consumption model based on the mechanics (i.e., the cutting force) that takes the tool wear into full consideration. Results of our numerous calibration physical drilling experiments will also be reported which convincingly validate the soundness and correctness of the proposed model. With this prediction model established, we will then report two optimization applications of the model in drilling process planning, one for drilling energy minimization and the other for drilling length maximization (or, equivalently, the maximization of tool usage). Results of the physical drilling experiments of the optimized solutions will then be reported, which clearly show the substantial improvement by the optimized machining parameters over the non-optimized ones in both energy reduction and maximization of tool usage.

2. Model of energy consumption considering tool wear in a drilling process

2.1. Drilling force model considering tool wear

The differential cutting forces in three-axis drilling by a twist drill (see Fig. 1) can be modelled as (Lee and Altintas (1996); Budak et al. (1996)):

$$dF_t = K_{tc}dA + K_{te}\Delta b \tag{1a}$$

$$dF_f = K_{fc}dA + K_{fe}\Delta b \tag{1b}$$

$$dF_r = K_{rc}dA + K_{re}\Delta b \tag{1c}$$

where K_{tc}, K_{fc}, K_{rc} (N/mm²) and K_{te}, K_{fe}, K_{re} (N/mm) are the specific cutting and edge force coefficients; dA (mm²) is the area of the differential chip lip being removed which can be calculated as $dA(z) = \Delta b \cdot h$, with h (mm) = $c/2\sin\kappa_t$, while κ_t is the taper angle and c is the spindle axial feed rate (mm/r); Δb is the chip width which can be calculated by $\Delta b = dz/\cos\kappa_t$; and dz is the chip height.

The differential cutting force components (dF_t, dF_f, dF_r) can be evaluated in the x, y, z directions as shown in Fig. 1 as follows:

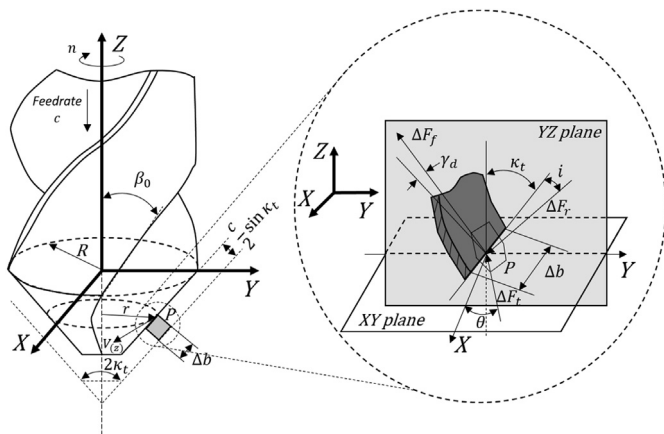


Fig. 1. A twist drill.

$$\begin{bmatrix} dF_x(z) \\ dF_y(z) \\ dF_z(z) \end{bmatrix} = \begin{bmatrix} -\cos\theta & \sin\gamma_d & -\sin i \\ -\sin\theta & -\cos\gamma_d \cdot \cos\kappa_t & \sin i \cdot \sin\gamma_d \cdot \cos\kappa_t \\ 0 & \cos\gamma_d \cdot \sin\kappa_t & \cos i \cdot \cos\kappa_t + \sin i \cdot \sin\gamma_d \cdot \sin\kappa_t \end{bmatrix} \times \begin{bmatrix} dF_t \\ dF_f \\ dF_r \end{bmatrix} \tag{2}$$

where θ is the angle between the x -axis and the cutting velocity ($V(z)$); γ_d is the angle between the tapered cutting edge and the component of the cutting speed in the y direction; and i is the oblique angle between the cutting velocity direction and the normal to the cutting edge.

While the tangential cutting force and z -axis force during the drilling process can be directly obtained by rotating the dynamometer, the axial and radial forces are difficult to measure physically, which though can be converted into the z -direction cutting force by the following formula:

$$dF_z = \left[\cos\gamma_d \cdot \sin\kappa_t \cdot K_{fc} + (\cos i \cdot \cos\kappa_t + \sin i \cdot \sin\gamma_d \cdot \sin\kappa_t) K_{rc} \right] dA + \left[\cos\gamma_d \cdot \sin\kappa_t \cdot K_{fe} + (\cos i \cdot \cos\kappa_t + \sin i \cdot \sin\gamma_d \cdot \sin\kappa_t) K_{re} \right] \cdot \Delta b \tag{3}$$

Since some of the parameters in the formulas are dynamic and difficult to obtain, the above formula can be simplified to:

$$dF_z = K_{zc}dA + K_{ze}\Delta b \tag{4}$$

where K_{zc} and K_{ze} are some coefficients, similar to the specific cutting and edge force coefficients.

Therefore, the cutting forces in three-axis drilling by a twist drill can be modelled as:

$$dF_t = K_{tc}dA + K_{te}\Delta b \tag{5a}$$

$$dF_z = K_{zc}dA + K_{ze}\Delta b \tag{5b}$$

In twist drilling, the tool wear appears in the form of flank wear in which the wear contact between the tool and the workpiece is no longer a single point but an area, as shown in the right in Fig. 2. Exactly because of this wear area, the cutting force is increased. Specifically, as shown in Fig. 2, when flank wear occurs, the wear area will produce additional forces in both the axial direction (F_{zw}) and the cutting direction (F_{tw}). The additional force in the axial direction (F_{zw}) is mainly caused by the rebound of the metal material, which can be determined by the rebound contact area and the stress of the rebound frictional contact surface, which can be

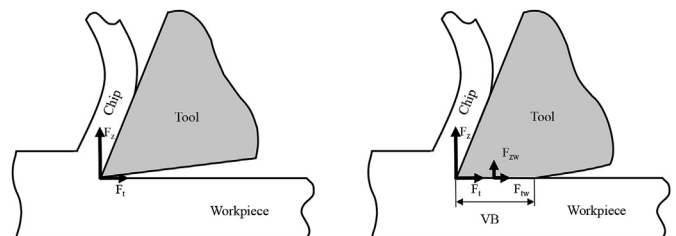


Fig. 2. A twist drill in a drilling process considering the tool wear.

expressed as:

$$dF_{zw} = \sigma \cdot VB \cdot \Delta b \quad (6)$$

where σ is the stress of the rebound frictional contact surface that can be expressed as:

$$\sigma = E\delta h \quad (7)$$

where E is the modulus of elasticity, δ is the material rebound rate, and h is the thickness of the cutting layer.

The additional force (F_{tw}) in the cutting direction is mainly caused by the friction between the tool and the workpiece, which is determined by the force between the two and their material properties. It can be expressed as:

$$\begin{aligned} dF_{tw} &= \mu(dF_z + dF_{zw}) = \mu(K_{zc}dA + K_{ze}\Delta b + \sigma \cdot VB \cdot \Delta b) \\ &= \mu(K_{zc}h + K_{ze} + E\delta h \cdot VB)\Delta b \end{aligned} \quad (8)$$

where μ is the sliding friction coefficient.

Therefore, the drilling force model considering the tool wear can be expressed as:

$$dF_t^w = K_{tc}dA + K_{te}\Delta b + \mu(K_{zc}h + K_{ze} + E\delta h \cdot VB)\Delta b \quad (9a)$$

$$dF_z^w = K_{zc}dA + K_{ze}\Delta b + E\delta h \cdot VB\Delta b \quad (9b)$$

The model can be simplified as:

$$dF_t^w = K_{tc}dA + (K_{te} + \Delta K_{tw})\Delta b \quad (10a)$$

$$dF_z^w = K_{zc}dA + (K_{ze} + \Delta K_{zw})\Delta b \quad (10b)$$

where ΔK_{tw} and ΔK_{zw} are variables related to the amount of flank wear (VB) (see Fig. 2), which can be expressed as:

$$\Delta K_{tw} = \mu(K_{zc}h + K_{ze} + E\delta h \cdot VB) \quad (11a)$$

$$\Delta K_{zw} = E\delta h \cdot VB \quad (11b)$$

2.2. The drilling cutting power model considering the tool wear

During a drilling process, the cutting energy consumption is generated along with the relative movement between the cutting edge and the workpiece. There are mainly two types of relative movement, one is due to the self-rotation of the drill, and the other due to the linear feed (in the axial direction). In order to accurately calculate the cutting energy consumption of drill, it is necessary to consider the energy consumption of these two types of motion, separately.

With respect to the self-rotation motion of drill, since dF_f and dF_r are perpendicular to the cutting velocity vector, no power is generated by them, and the differential powers (W) consumed at each infinitesimal cutting edge in the tangential, feed, and radial directions are respectively:

$$dP_{rotation,t} = dF_t^w \cdot V(z) \quad (12a)$$

$$dP_{rotation,f} = 0 \quad (12b)$$

$$dP_{rotation,r} = 0 \quad (12c)$$

where $V(z)$ (m/s) is the cutting speed. The total power consumed at

the infinitesimal cutting edge due to the spindle rotational motion can then be expressed as

$$dP_{rotation} = dF_t^w \cdot V(z) \quad (13)$$

Next, with respect to the linear feed motion, as dF_t is perpendicular to the feed direction, no power is generated by it, and the differential powers are

$$dP_{feed,t} = 0 \quad (14a)$$

$$dP_{feed,f} = dF_f^w \cdot \cos\gamma_d \cdot \sin\kappa_t \cdot f / 60000 \quad (14b)$$

$$dP_{feed,r} = dF_r^w (\cos i \cdot \cos\kappa_t + \sin i \cdot \sin\gamma_d \cdot \sin\kappa_t) \cdot f / 60000 \quad (14c)$$

where f (m/s) is the feed rate. The total power consumed at the infinitesimal cutting edge due to the feed motion can then be expressed as

$$\begin{aligned} dP_{feed} &= \left[dF_f^w \cdot \cos\gamma_d \cdot \sin\kappa_t \right. \\ &\quad \left. + dF_r^w (\cos i \cdot \cos\kappa_t + \sin i \cdot \sin\gamma_d \cdot \sin\kappa_t) \right] \cdot f / 60000 \end{aligned} \quad (15)$$

According to Eq. (2), Eq. (15) can then be expressed as

$$dP_{feed} = dF_z^w(z) \cdot f / 60000 \quad (16)$$

Finally, combining both Eq. (13) and Eq. (16), the instantaneous power consumption due to cutting can then be modelled as:

$$\begin{aligned} P_{cutting}^w &= P_{feed} + P_{rotation} = \int dP_{feed} + \int dP_{rotation} \\ &= f / 60000 \cdot \int dF_z^w(z) + \int V(z) \cdot dF_t^w(z) \end{aligned} \quad (17)$$

2.3. The total drilling power model considering the tool wear

Although in a drilling process the power consumption model is extremely complex, according to (Hu et al., 2012), the total power flow of machining on any machine tool can be separated into three parts: the idle power P_{idle} , the cutting power $P_{cutting}$, and the auxiliary power $P_{auxiliary}$ (load loss). That is, we have:

$$P_{total} = P_{idle} + P_{cutting} + P_{auxiliary} \quad (18)$$

where the idle power P_{idle} can be expressed as a function related to the spindle speed n , i.e., $P_{idle} = g(n)$ (Li et al. (2013) and (Ma et al., 2017)), and the auxiliary power $P_{auxiliary}$ can be expressed as a linear ($P_{auxiliary} = C_0 P_{cutting}$) or, more accurately, quadratic ($P_{auxiliary} = C_0 P_{cutting} + C_1 P_{cutting}^2$) function of the cutting power (Hu et al. (2010, 2012)).

Thus, at the steady drilling state, the total drilling power consumption can be expressed as:

$$P_{total} = P_{idle} + P_{cutting} + P_{auxiliary} = P_{idle} + P_{cutting}^w + f(P_{cutting}^w) \quad (19)$$

3. Energy consumption model calibration experiments

3.1. Setup and drilling parameters of the experiments

The physical drilling experiments were carried out on YH850Z, which is a three-axis machine tool with a spindle power of 7.5 kW. The material of the workpiece is GH4169 and the raw stock to drill is a brick with dimensions of 190 mm × 120 mm × 16 mm. The tool used in the machining experiments is a twist drill with a diameter of 10 mm. The cutting condition is wet cutting. Table 1 gives the drilling parameters.

A total of 12 combinations were selected. Under each set of cutting parameters, the tool wear was inspected after each drilling of 5 holes, until it reached its failure threshold. During the experiments, all the force profiles were measured with a Kistler 9123C rotary dynamometer (Fig. 3(a)). For power measurement, a HIOKI clamp on power logger PW3360 was used (Fig. 3(b)). The power profile of the machine tool was measured at a sampling frequency of 1 Hz. The tool wear data were measured using a microscope (Fig. 3(c)).

3.2. Cutting force coefficients and wear coefficient calibration

Since the cutting force coefficients change with the amount of tool wear, the force data obtained at the very beginning of drilling (i.e., after drilling the first hole of 16 mm length) using a brand new tool are used to perform the basic calibration of the cutting force coefficients. As shown in Fig. 4, it can be seen that the change of the spindle speed has little effect on the change of the cutting force coefficients. Therefore, the influence of the spindle rotation speed on the cutting force coefficients can be ignored. Based on the data from the experiments, the cutting force coefficients were calculated as:

$$K = [K_{tc} \ K_{te} \ K_{zc} \ K_{ze}]^T = [5120.3 \ 134.0 \ 5200.6 \ 334.9]^T$$

Using the obtained cutting force coefficients, the force profiles under different pairs of (n, f) can be predicted (Han et al., 2018). Fig. 5 shows some of the prediction results in comparison with the experimental data. From the figure, it can be concluded that our cutting force prediction results are generally acceptable, indicating that the coefficients K can be reliably used.

After obtaining a reliable set of basic cutting force coefficients, the wear coefficients ΔK generated by the flank wear were calibrated. First, the relationship between the amount of tool wear VB and the number N of drilled holes (with each hole having a fixed and same length) is established by the experimental data (as shown in Fig. 6), which can be expressed as:

$$VB(N) = \sum_{i=0}^N a_i N^i \quad (20)$$

The above equation thus gives the relationship between the amount of flank wear VB and the number N of drilled holes. Since all the holes have the same length (16 mm), ignoring the minor effect of tool entry, the equation actually gives out VB as a function of the

Table 1
Cutting (drilling) parameters for the calibration experiments.

n [rpm]	c [mm/r]
550	0.08 0.11 0.14 0.17
700	0.08 0.11 0.14 0.17
850	0.08 0.11 0.14 0.17

length of drill.

At the same time, although the curve shapes of tool wear – length of drill under different machining parameters are different (Fig. 6), we still can find some rules (as further exemplified in Fig. 7). As shown in Fig. 7(a), when the feed rate is fixed (e.g., $c = 0.11$ mm/r), the tool wear VB increases with the increase of the spindle speed n , indicating that a larger spindle speed n would lead to a shorter tool life (at least for the tested range of n in 550 rpm–850 rpm). On the other hand, as revealed from Fig. 7(b), when the spindle speed is fixed (e.g., $n = 550$ rpm), the influence of the feed rate on the curve shape of tool wear – length of drill is relatively small.

Using the established tool wear (VB) function of Eq. (20), the wear coefficients ΔK can be calculated based on the experimentally measured cutting force and the calculated basic cutting force. Specific to our setting of experiments, the relationship between the wear coefficients ΔK and the tool wear VB can be expressed as (see Fig. 8):

$$\Delta K_{tw} = 0.5571VB - 7.6583 \quad (21a)$$

$$\Delta K_{zw} = 0.2309VB - 52.994 \quad (21b)$$

After obtaining the above functions, under fixed machining parameters (n, f) and using a brand new tool (i.e., with a zero flank wear) to start with the first hole to drill, the cutting force on the tool when drilling the i -th hole can be calculated according to Eq. (10). The comparison between the cutting forces obtained by our tool wear prediction model and the experimentally measured is given in Fig. 9, which shows a very close agreement, thus validating the prediction model. Next, with the cutting force accurately predicted, the due cutting power can be accordingly accurately calculated, as detailed next.

3.3. Energy consumption model calibration

In the non-cutting state, by changing the spindle speed n and physically measuring the corresponding P_{total} , the idle power P_{idle} at different spindle speeds can be obtained. Fig. 10 draws the obtained relationship between P_{idle} and the spindle speed n . By using the standard linear least squares (LLS) fitting method, the following $P_{idle} - n$ curve is established:

$$P_{idle} = 0.0003n^2 + 0.0524n + 1221 \quad (23)$$

Table 2 lists the data from the drilling experiments (in each of which a brand new tool was used), where P_{total} is the actual total power recorded by the power logger, while P_{idle} and $P_{cutting}$ are respectively calculated (i.e., predicted) by Eq. (23) and Eq. (17). Based on them, with Eq. (18), i.e., $P_{auxiliary} = P_{total} - P_{idle} - P_{cutting}$, the relationship between the auxiliary power $P_{auxiliary}$ and the cutting power $P_{cutting}$ can be derived, as shown in Fig. 11, which shows a near-linearity relationship given as:

$$P_{auxiliary} = 0.1336P_{cutting} \quad (24)$$

Finally, substituting Eq. (24) into Eq. (19), the total power model can be expressed by the equations for P_{idle} and $P_{cutting}$, i.e., Eq. (23) and Eq. (17), when the machining parameters are determined. That is,

$$P_{total} = P_{idle} + 1.1336P_{cutting}^w \quad (25)$$

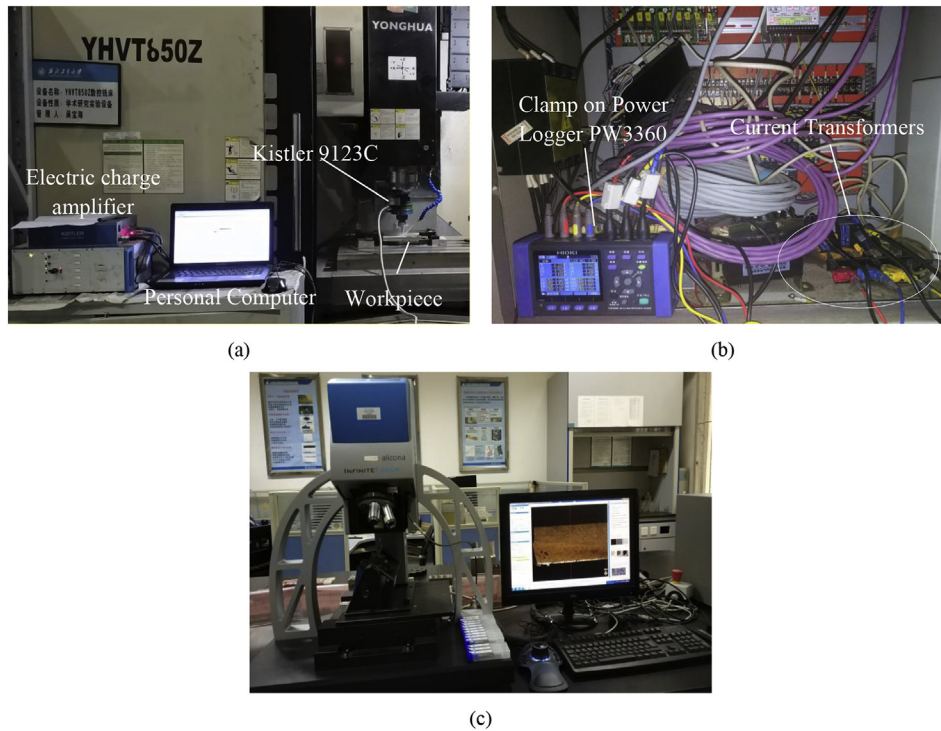


Fig. 3. The experiment setup: (a) the fixture of the workpiece and the force signal processing and collection; (b) the installation of the power meter; (c) the setup for tool wear measurement.

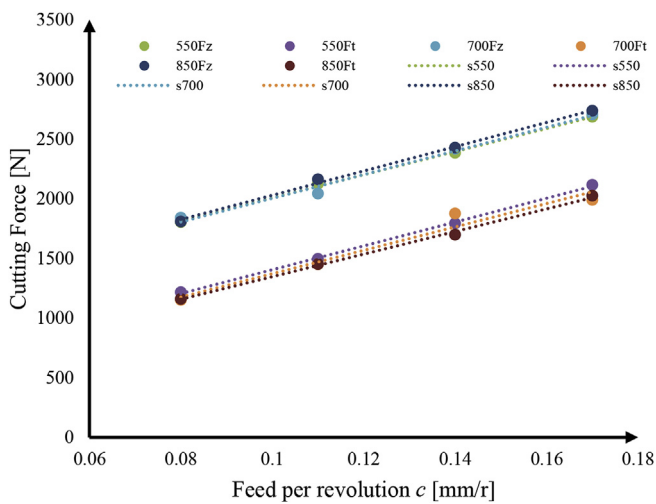


Fig. 4. Relationship between the feed per revolution c and the cutting force.

4. Model validations and discussion

In this section, the proposed energy model considering the tool wear is validated by more physical drilling experimental data, analysed, and also compared with the one that ignores the tool wear.

4.1. Validation of energy prediction model

In Fig. 12, under three different drilling parameters (n, f), i.e., that of No. 2, No. 7, and No. 12 from Table 2, we show the experimental data of the total power, the predicted power ignoring the tool wear (predict), and the predicted power considering the tool wear

(predict-wear). First of all, the experimental data in the figure validate that our established total power model considering the tool wear closely agrees with the actually recorded power consumption during the drilling experiments. Then, the actual recorded data unequivocally confirm that the tool wear indeed increases the power consumption, and it becomes more and more severe with the increase of the drilling length. For example, as shown in Fig. 12(b), for the setting of $f = 98$ mm/min and $n = 700$ rpm, after having drilled 50 holes, the actual recorded power consumption is more than 2240 W, while a lower and incorrect 2130 W would be predicted by our first energy model that ignores the tool wear.

Next, under the 12 drilling parameter pairs (n, f) given in Table 2, we performed physical drilling experiments, recorded the cutting force and total power consumption for each hole processed, and then compared the recorded cutting forces and the total power consumption respectively with the ones predicted by our established cutting force prediction models (with and without considering the tool wear) and the total power prediction models (with and without considering the tool wear), and Table 3 lists their respective average normalized errors. As can be seen in the table, when considering the tool wear, our prediction model for the tangential drilling force, i.e., F_t^w , agrees much more closely with the actual data than the one ignoring the tool wear (F_t), or specifically, it is 2.19% vs. 7.37%. On the other hand, as already explained earlier, as the tool wear mainly affects the tangential drilling force, our cutting force models for the axial drilling force with and without considering the tool wear, i.e., F_z^w and F_z respectively, more or less are the same, i.e., 2.70% vs. 2.73% in terms of the error measure. In the same light, as power is induced by the cutting force, ignoring the tool wear in power calculation would miss the power due to the cutting force induced by the tool wear, thus adding more error to the estimate of power. Specifically, as also shown in Fig. 13, from the data of 12 physical drilling tests, on average, our power prediction model P^w that considers the tool wear deviates from the actually recorded

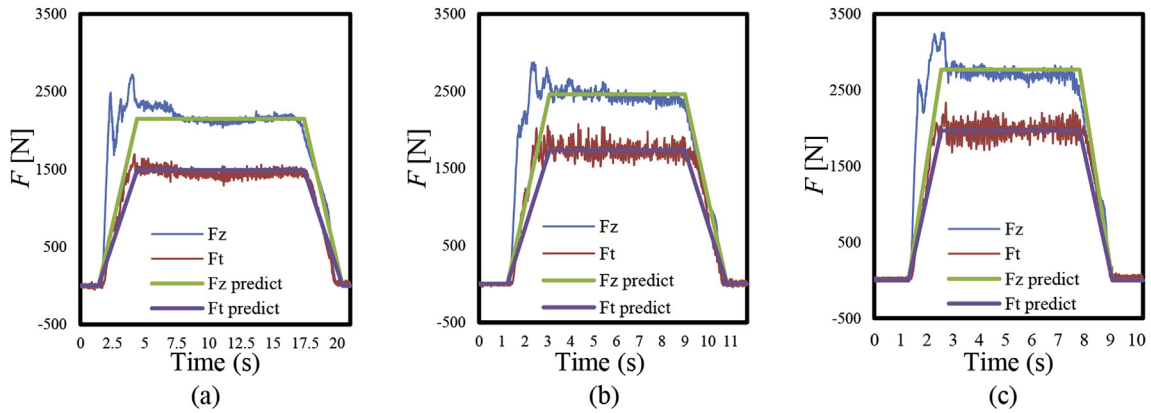


Fig. 5. Cutting force prediction in the drilling experiments under different cutting parameters: (a) $n = 550$ rpm, $f = 60.5$ mm/min; (b) $n = 700$ rpm, $f = 98$ mm/min; (c) $n = 850$ rpm, $f = 144.5$ mm/min.

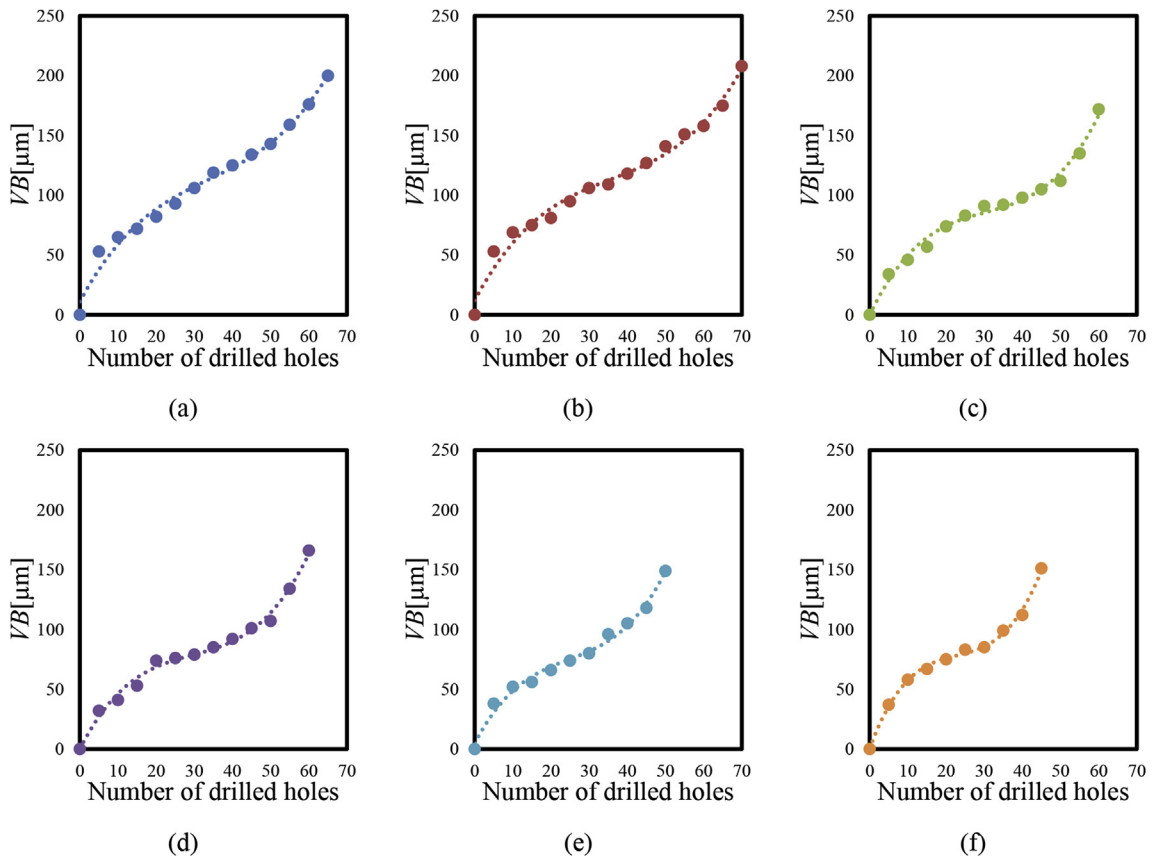


Fig. 6. Relationship between the number of drilled holes and the tool wear VB under different drilling parameters: (a) $n = 550$ rpm, $f = 44$ mm/min; (b) $n = 550$ rpm, $f = 60.5$ mm/min; (c) $n = 700$ rpm, $f = 77$ mm/min; (d) $n = 700$ rpm, $f = 98$ mm/min; (e) $n = 850$ rpm, $f = 119$ mm/min; (f) $n = 850$ rpm, $f = 144.5$ mm/min.

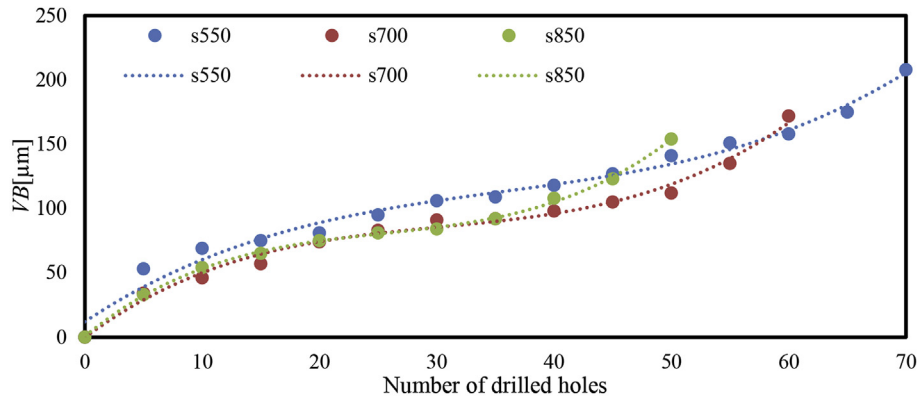
power by only 0.99%, while that (i.e., P) without considering the tool wear has an error of 2.97%.

4.2. Validation of the tool wear prediction model

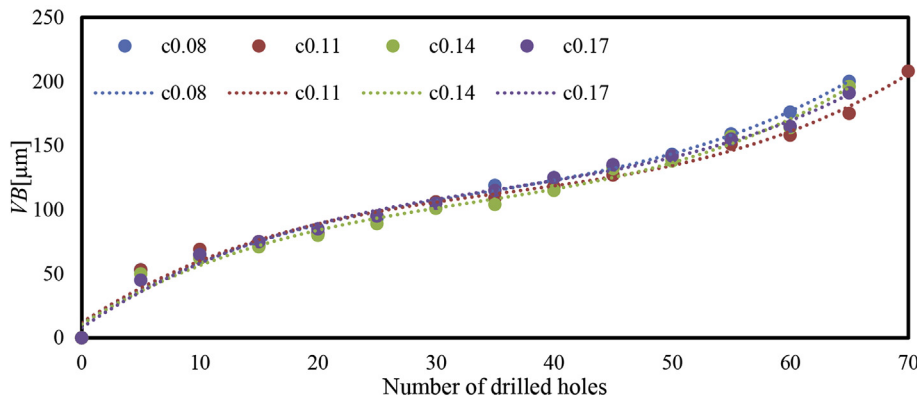
The proposed prediction models for drilling cutting forces and the power consumption can be used to predict the tool wear as a function of the length of drill (i.e., the number of holes to drill, assuming that all the holes have the same length). Specifically, under any fixed drilling parameters (n, f), after having drilled a certain length, we can use our power prediction model to predict

the total power consumption at that time; then, based on our cutting force model, we predict the cutting power and the axial and tangential cutting forces that consider the tool wear, as well as the basic cutting power and basic cutting forces that ignore the tool wear. The difference is then the change caused by the tool wear VB , and it can be calculated from the formula of the wear coefficients, i.e., either Eq. (21a) or Eq. (21b).

To validate the just prescribed prediction model of tool wear, under the three different drilling parameters (n, f) of test No. 2, No. 7, and No. 12 from Table 2, we performed physical drilling experiments and recorded the power readings and measured the



(a) Relationship between the tool wear and the spindle speed n ($c = 0.11$ mm/r)



(b) Relationship between the tool wear and the feed rate c ($n = 550$ rpm)

Fig. 7. Relationship graphs of tool wear – spindle speed and tool wear – feed rate.

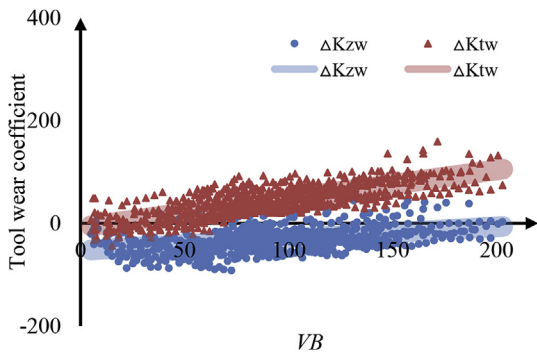


Fig. 8. Relationship between VB and the tool wear coefficients.

corresponding tool wear VB 's at the sample lengths of drill. E.g., under test No. 7, after 5 holes had been drilled, we stopped the drilling, used a microscope to measure the tool wear VB , and then read the power value at the power logger. Meanwhile, using these measured tool wear VB 's, we calculated their corresponding predicted power based on our cutting force and power model. The comparison data are given in Fig. 14; from which we can draw the following points:

- (1) Our prediction model for the power in general agrees with the physical experimental data.
- (2) The total power consumption increases with the increase of the tool wear VB .

- (3) With respect to a same threshold of VB , the larger the feed rate f or spindle rpm n , the larger the power consumption is when the threshold is reached; e.g., when $VB = 100 \mu\text{m}$ is reached, with respect to the (n, f) of (550 rpm, 60.5 mm/min) and (850 rpm, 144.5 mm/min), the corresponding total power consumptions are 1865 W and 2600 W, respectively.

It should be noted that in the experiments of Fig. 14, the predicted power values are calculated using the actual measured tool wear VB 's and that is why they are said to be *queasily predicted*. On the other hand, we have already established the relationship between the total power and the length of drill (see Fig. 12). This means that, given the length of drill (i.e., the number of holes that have been drilled), we can use it to directly predict the corresponding total power which can then be used to inversely calculate the corresponding VB . Naturally, we call this type of prediction a *full prediction* – no physical data are needed. In Fig. 15, we show the comparison between the power– VB graphs of full prediction and the physical experimental data. As clearly seen in Fig. 15, the results of full prediction closely match the physical experimental data, which in turn implies the correctness of the proposed power model and cutting force model considering the tool wear.

As a final validation work, for each of the 12 (n, f) 's from Table 2, we performed physical drilling experiments in which, after every 5 holes had been drilled, we stopped the drilling, measured the tool wear VB , and then resumed the drilling. These experimental data were then compared with the VB 's that were calculated by our full prediction model, as shown in Table 4. (In the table, whenever a blank, it means the tool wear VB at the time of measurement had already reached the $150 \mu\text{m}$ tool wear threshold.) The comparison

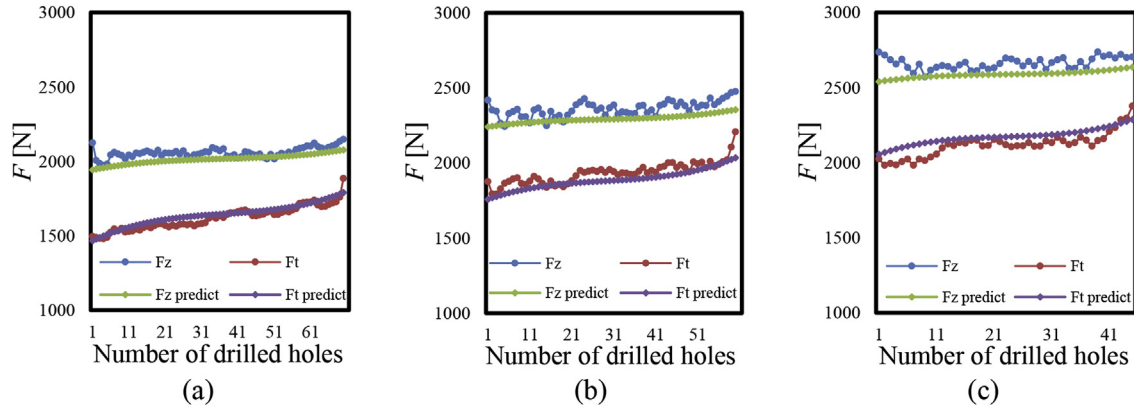


Fig. 9. Cutting force prediction considering the tool wear under different cutting parameters: (a) $n = 550$ rpm, $f = 60.5$ mm/min; (b) $n = 700$ rpm, $f = 98$ mm/min; (c) $n = 850$ rpm, $f = 144.5$ mm/min.

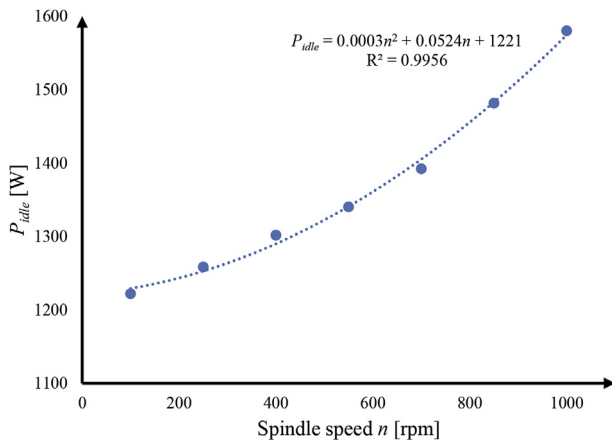


Fig. 10. The idle power at different spindle speeds.

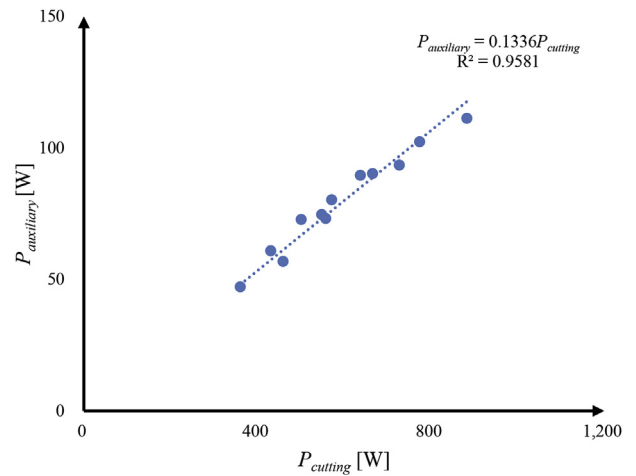


Fig. 11. The relationship between the auxiliary power and the calculated cutting power.

Table 2
The recorded total power (P_{total}) and the calculated idle power (P_{idle}) and cutting power ($P_{cutting}$).

No.	n [rpm]	f [mm/min]	P_{total} [W]	P_{idle} [W]	$P_{cutting}$ [W]
1	550	44	1750.0	1340.6	360.9
2	550	60.5	1837.4	1340.6	430.9
3	550	77	1937.0	1340.6	501.1
4	550	93.5	2001.8	1340.6	571.5
5	700	56	1906.1	1404.7	459.3
6	700	77	1988.8	1404.7	548.4
7	700	98	2117.4	1404.7	637.8
8	700	119	2217.9	1404.7	727.4
9	850	68	2067.9	1482.3	557.7
10	850	93.5	2217.5	1482.3	665.9
11	850	119	2354.8	1482.3	774.4
12	850	144.5	2474.4	1482.3	883.2

data show that the maximum average error of the fully predicted tool wear under various processing parameters (n, f) is less than 8% in a large drilling range of 0 mm–1120 mm, while the total average error is 5.74%. However, if we removed the initial length of drill from the calculation, the error would be much smaller. This is because the tool wear is intense at the beginning of the tool's use, which leads to irregular and drastic changes in the cutting force (even the physically measured cutting force showed an irregular decreasing trend in the beginning of drilling, as shown in Fig. 9). As a result, our theoretical tool wear prediction model has a relatively

large error at the initial stage of drill (i.e., for the first 10 holes, or 160 mm). However, as the main purpose of tool wear prediction is to accurately predict the normal tool wear so to achieve a timely replacement of the tool, and the initial stage of tool wear is not the main predictor, this prediction error at the initial stage of wear can be simply ignored. As the tool enters its normal wear phase, the tool wear becomes more stable, and our tool wear prediction error is significantly reduced to a relatively accurate range, e.g., an average of only 1.41% for the 30th – 60th holes in test No. 1.

5. Applications

As the final part of this research work, in this section we present two applications of our established prediction models for the tool wear and power consumption in drilling.

5.1. Maximize the length of drill under a given threshold of tool wear

Under any fixed setup of drilling, our prediction model for the tool wear establishes a relationship between the length of drill L and the drilling parameters (n, f) with respect to any given tool wear threshold VB . Let $L_{VB}(n, f)$ denote such a function. As a concrete example, under our setup of drilling given in Section 3.1,

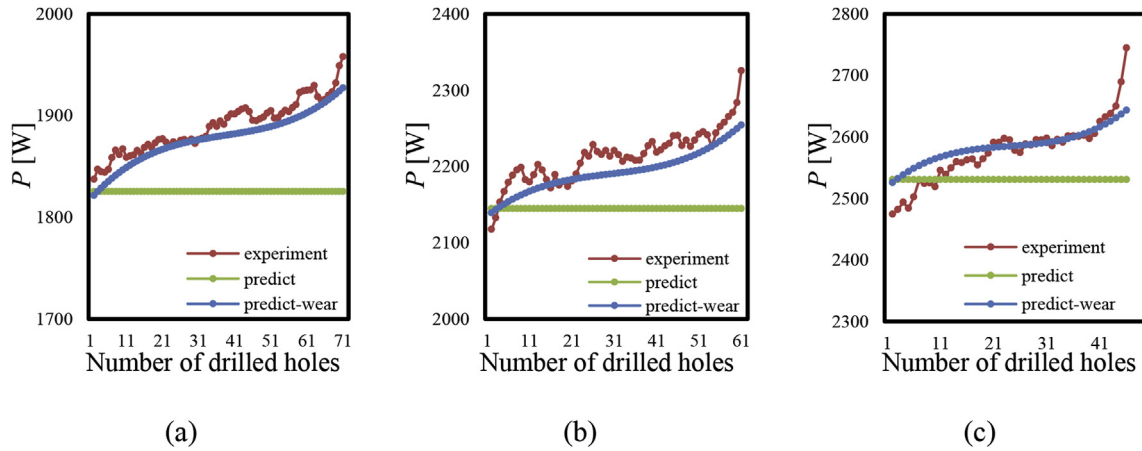


Fig. 12. Total power prediction in the drilling experiments under different cutting parameters: (a) $n = 550$ rpm, $f = 60.5$ mm/min; (b) $n = 700$ rpm, $f = 98$ mm/min; (c) $n = 850$ rpm, $f = 144.5$ mm/min.

Table 3
Comparison of the prediction models with and without considering the tool wear.

Test No.	F_z	F_t	F_z^w	F_t^w	P	P^w
1	2.35%	12.3%	3.16%	1.78%	4.02%	1.12%
2	2.17%	8.48%	2.13%	1.73%	3.39%	0.97%
3	1.85%	6.95%	2.25%	1.54%	3.24%	0.83%
4	3.15%	4.81%	0.68%	2.82%	3.50%	1.00%
5	3.67%	8.94%	2.93%	1.27%	3.49%	1.00%
6	5.31%	6.94%	1.82%	2.49%	2.34%	0.83%
7	2.08%	8.27%	2.87%	2.44%	3.12%	0.97%
8	3.34%	4.36%	1.65%	1.53%	1.10%	0.84%
9	3.15%	11.0%	5.20%	2.89%	3.57%	0.98%
10	2.68%	8.50%	3.44%	1.68%	4.19%	1.75%
11	1.47%	3.87%	3.44%	3.22%	1.51%	0.80%
12	1.52%	3.69%	2.76%	2.85%	2.18%	0.78%
Average prediction error	2.73%	7.37%	2.70%	2.19%	2.97%	0.99%

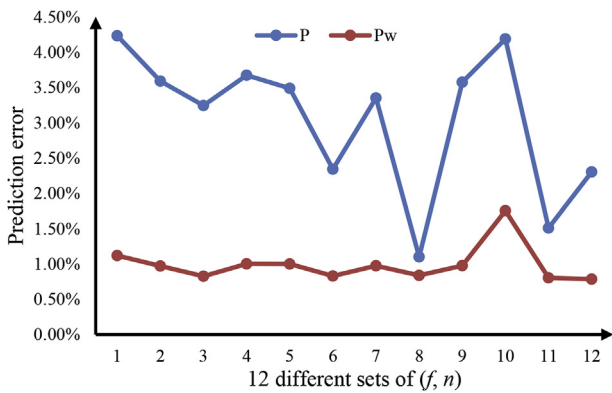


Fig. 13. Comparison of the prediction errors of the power models with and without considering the tool wear.

when the tool wear threshold VB is set at $150 \mu\text{m}$, Fig. 16 draws the corresponding length of drill function $L_{VB=150\mu\text{m}}(n, f)$. Explicitly, given any pair of (n, f) within the domain $[550 \text{ rpm}, 850 \text{ rpm}] \times [44 \text{ mm/min}, 144 \text{ mm/min}]$, function $L_{VB=150\mu\text{m}}(n, f)$ gives the corresponding length of drill when the tool wear reaches the threshold $150 \mu\text{m}$. As can be seen in Fig. 16, $L_{VB=150\mu\text{m}}(n, f)$ resembles an inverted saddle shape, which naturally implies the plausibility of optimizing n and/or f to maximize L .

For the specific function $L_{VB=150\mu\text{m}}(n, f)$ of Fig. 16, we numerically

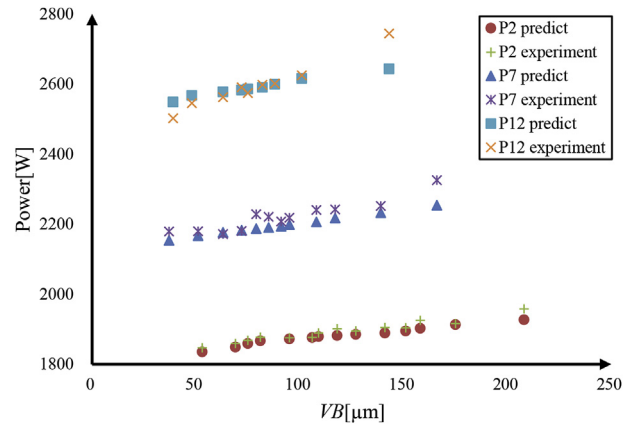


Fig. 14. Comparison between the power- VB graphs that are acquired from the physical drilling experiments and queasily predicted respectively.

calculated the optimal (n, f) which is found to be around $(n^*, f^*) = (685 \text{ rpm}, 92 \text{ mm/min})$. As a benchmark to compare, we also picked an arbitrary pair $(n^B, f^B) = (850 \text{ rpm}, 44 \text{ mm/min})$. We have $L_{VB=150\mu\text{m}}(n^*, f^*) = 960 \text{ mm}$ and $L_{VB=150\mu\text{m}}(n^B, f^B) = 688 \text{ mm}$. Under (n^*, f^*) and (n^B, f^B) , we then performed physical drilling for a length of drill of 960 mm and 688 mm respectively, and then measured the tool wear VB . Meanwhile, we also recorded the total energy consumptions of the two drills. Table 5 below lists the experimental results. As clearly validated in the table, our prediction data in both tool wear and energy consumption closely match their respective physical experimental results. Moreover, the experimental results have convincingly confirmed our intended optimization objective: comparing to the arbitrarily chosen (n^B, f^B) , the optimized (n^*, f^*) not only increases the total length of drill by 40% but also at the same time reduces the total energy consumption by 34%.

Sometimes, due to different process constraints, only one of n and f is free to change while the other is predetermined. For example, suppose the spindle rpm n is predetermined and in Fig. 17 we draw the function $L_{VB=150\mu\text{m}}(f)$ at three different n 's. Take $n = 550 \text{ rpm}$ as an illustrative example. Intuitively, to increase the productivity, a larger feed rate f is preferred, e.g., 140 over 70 mm/min , as the former doubles the latter. However, at $f = 140 \text{ mm/min}$, the tool will have to be replaced by a new one after only a length of 700 mm has been drilled; or in other words, a brand new tool can drill only 44 holes. On the other hand, at the much smaller

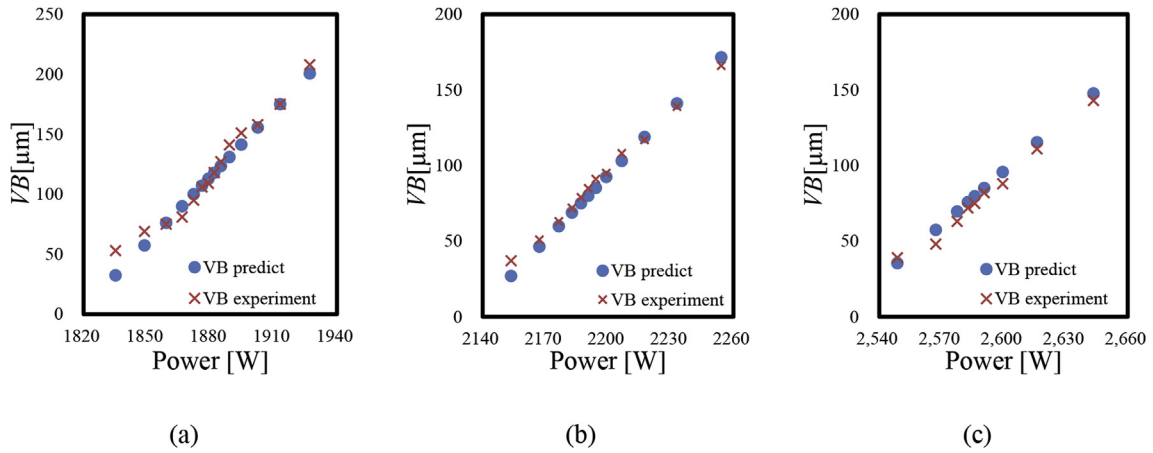


Fig. 15. The fully predicted tool wear versus the measured tool wear: (a) $n = 550$ rpm, $f = 60.5$ mm/min; (b) $n = 700$ rpm, $f = 98$ mm/min; (c) $n = 850$ rpm, $f = 144.5$ mm/min.

Table 4
Tool wear full prediction error under various machining parameters (n, f).

Hole no.	No. 1	No. 2	No. 3	No. 4	No.5	No. 6	No. 7	No. 8	No. 9	No.10	No.11	No.12
5	39.8%	39.1%	38.5%	29.4%	21.5%	14.7%	27.1%	32.8%	14.1%	3.79%	24.8%	9.01%
10	12.7%	17.0%	12.3%	12.8%	1.85%	8.63%	9.02%	8.43%	12.3%	1.59%	7.30%	19.7%
15	5.02%	1.55%	1.57%	1.06%	2.51%	13.1%	5.01%	8.44%	3.02%	2.65%	9.05%	10.6%
20	9.49%	11.2%	6.42%	6.20%	3.05%	0.19%	4.33%	8.49%	2.57%	0.06%	5.07%	5.32%
25	7.98%	5.28%	6.34%	6.56%	1.88%	1.89%	4.95%	6.76%	2.24%	0.43%	1.63%	6.32%
30	2.59%	1.17%	0.83%	4.56%	0.02%	0.13%	5.84%	0.46%	4.75%	2.50%	1.03%	3.81%
35	2.56%	3.51%	3.78%	1.81%	1.79%	1.55%	6.25%	5.85%	0.18%	2.11%	7.94%	8.80%
40	1.41%	0.08%	0.78%	0.62%	0.12%	0.51%	2.65%	0.71%	6.11%	1.18%	4.72%	3.91%
45	1.64%	2.68%	7.90%	1.96%	3.86%	0.59%	4.52%	0.59%	2.92%	3.25%	0.01%	3.26%
50	0.10%	7.07%	4.68%	0.41%	0.08%	0.73%	1.54%	7.46%		2.15%	3.08%	
55	0.90%	6.40%	7.53%	0.67%	1.82%	1.09%	1.51%	6.97%				
60	0.67%	1.51%	0.17%	5.37%	0.88%	0.11%	3.37%	0.21%				
65	1.40%	0.01%	3.90%	3.22%								
70		3.50%										
Average Error	6.64%	7.15%	7.28%	5.74%	3.28%	3.60%	6.34%	7.26%	5.35%	1.97%	6.46%	7.86%

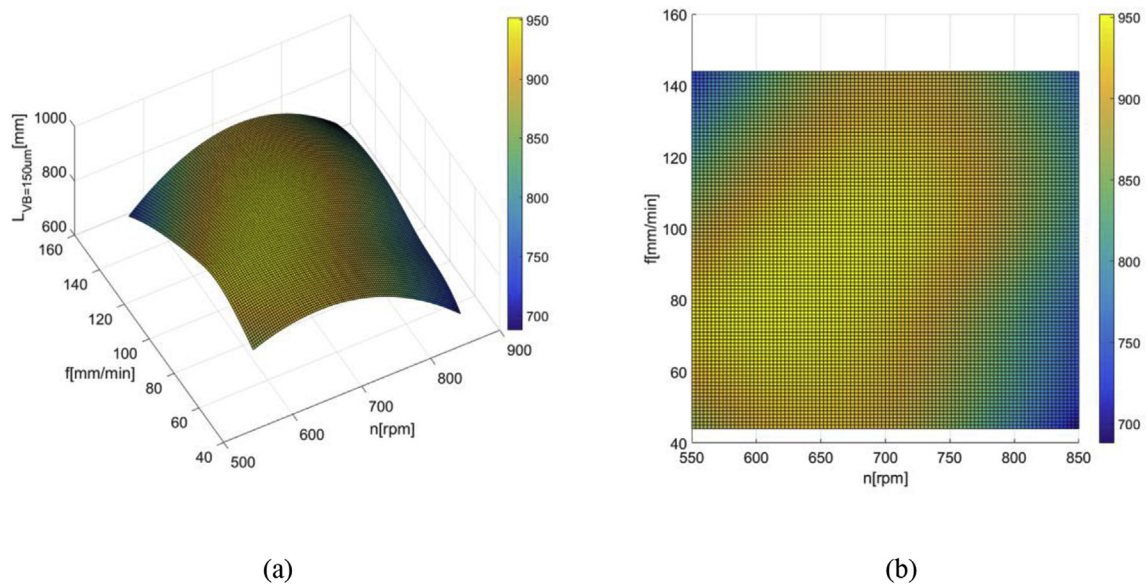


Fig. 16. Relationship between the drilling parameters (n, f) and length of drill L .

Table 5
Comparison of energy consumption and VB prediction with the actual experimental data.

	$L(\text{mm})/\text{hole no.}$	Experiment $VB(\mu\text{m})$	Predict $VB(\mu\text{m})$	Error(VB)	Experiment $E(\text{J})$	Predict $E(\text{J})$	Error(E)
(n^*, f^*)	960/60	147.3	150.5	2.12%	3.70E+06	3.57E+06	3.51%
(n^B, f^B)	688/43	145.1	149.9	3.31%	5.64E+06	5.41E+06	4.08%

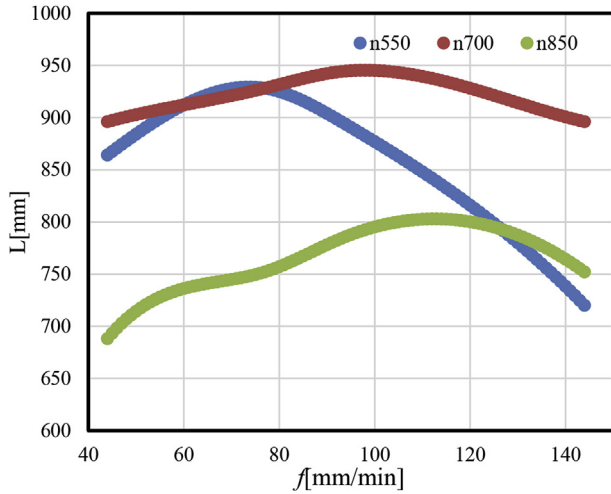


Fig. 17. Relationship between feed rate f and tool life L under different spindle rpm n .

$f = 70$ mm/min, 58 holes (i.e., length of drill = 928 mm) can be drilled by a single tool before its replacement, which is a 32% reduction in the cost of tool.

5.2. Minimum energy consumption of drilling under a given length of drill

Akin to the length function $L_{VB}(n, f)$, our prediction models for the tool wear and power consumption also establish a relationship between the total energy consumption E and the drilling parameters (n, f) with respect to any given length of drill L . Specifically, we will use $E_L(n, f)$ to represent this energy function, e.g., $E_{800\text{mm}}$ (650 rpm, 980 mm/min) stands for the total energy consumption

after drilling a length of 800 mm using a single tool with $(n, f) = (650 \text{ rpm}, 980 \text{ mm/min})$. With $E_L(n, f)$ available for any valid L , the following optimization problem naturally rises: given a tool wear threshold (e.g., $VB = 150 \mu\text{m}$) and a length to drill (e.g., $L = 800 \text{ mm}$), what should be the optimal pair (n, f) that will minimize the function $E_L(n, f)$?

As a concrete example, under the setup of drilling given in Section 3.1 and the tool wear threshold $VB = 150 \mu\text{m}$, suppose we want to find the most energy-efficient pair (n, f) to drill 58 holes (length of drill $L = 928 \text{ mm}$) without changing the tool. Fig. 18(a) draws the corresponding total energy consumption function $E_{L=928\text{mm}}(n, f)$. With the help of function $L_{VB=150\mu\text{m}}(n, f)$ as shown in Fig. 16, we can then numerically find out the safety domain in (n, f) in which the tool wear VB will not exceed the threshold $150 \mu\text{m}$ after 58 holes are drilled, as shown in Fig. 18(b), where the red coloured curve is the identified boundary of the safety domain. As both functions L_{VB} and E_L are continuous, it is obvious that the optimal (n, f) must lie on the boundary of the safety domain, i.e., on the red coloured curve in Fig. 18(b). Next, on this boundary curve, we numerically found the optimal (n, f) to be around $(n^{\text{min}}, f^{\text{min}}) = (685 \text{ rpm}, 120 \text{ mm/min})$. As a benchmark to compare, we also numerically identified another pair $(n^{\text{max}}, f^{\text{max}}) = (643 \text{ rpm}, 56 \text{ mm/min})$ that maximizes the function $E_{L=928\text{mm}}(n, f)$. The $E_{L=928\text{mm}}$ values of these two (n, f) 's are also shown in Fig. 18(a). Finally, under $(n^{\text{min}}, f^{\text{min}})$ and $(n^{\text{max}}, f^{\text{max}})$ respectively, we performed physical drilling for a length of drill of 928 mm, and then recorded the total energy consumption. Table 6 lists the experimental as well as the prediction results.

As revealed from Table 6, there is a significant difference in the total energy consumption for drilling 58 holes using these two different sets of parameters. Specifically, based on the real experimental data, the total energy consumption of the most energy-efficient $(n^{\text{min}}, f^{\text{min}})$ is only 52.8% of that of $(n^{\text{max}}, f^{\text{max}})$, i.e., 2.83/5.35. The data also demonstrate that our predicted amounts of total

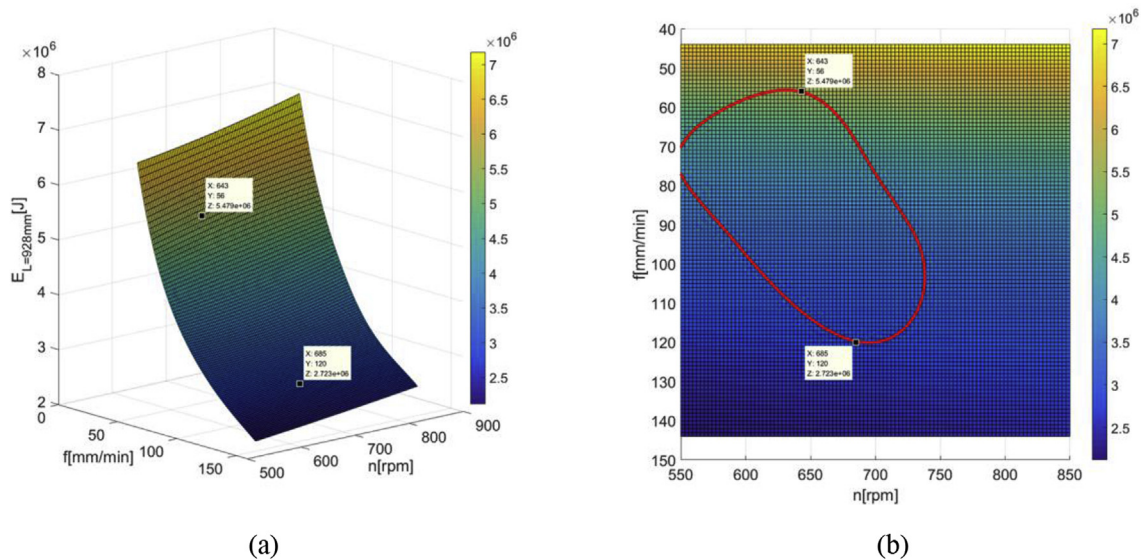


Fig. 18. Relationship between (n, f) and the total energy consumption: (a) total energy as a function of (n, f) ; (b) the safety domain in (n, f) .

Table 6

Predicted and experimental total energy consumption after 58 holes are drilled.

	L(mm)/Hole No.	Experiment E(J)	Predicted E(J)	Error
(n^{\min}, f^{\min})	928/58	2.83E+06	2.72E+06	3.89%
(n^{\max}, f^{\max})	928/58	5.35E+06	5.48E+06	2.43%

energy consumption are very close to the real data, which further validates the correctness and efficacy of the tool wear and power prediction models that we have established in this paper.

6. Conclusions

We have presented a mechanics based model for predicting the power consumption of drilling operations. The motivation behind our work is that currently all the existing energy models for machining ignore the effect of tool wear, while tool wear is particularly worrisome in drilling and it induces extra and large cutting force and thus more energy consumption. Our power model takes the tool wear into full consideration and thus is more accurate in predicting the drilling power consumption. The physical calibration drilling experiments performed by us have clearly validated the accuracy of our prediction model and verified that drilling power prediction without considering the tool wear is inaccurate. Two applications of the presented power prediction model in drilling process planning are then presented, one in minimizing the average power consumption per unit length of drill and the other in maximizing the tool usage before its replacement. Physical drilling experiments were also performed by us to compare the optimized drilling operations with some benchmarks (i.e., non-optimized), and the comparison results firmly show the efficacy of the presented power prediction model in helping significantly reducing the drilling energy consumption and increasing the tool usage.

About the potential future research on the subject, on the one hand, we plan to consider more influencing factors regarding the drilling energy consumption, such as different types of drilling tools, the drilling hole diameter, and the cooling condition. On the other hand, we plan to extend the proposed power consumption model to the general process of milling of freeform surfaces. Admittedly, when planning for milling a freeform surface, many more process or machining parameters will be involved, such as the number of passes of semi-finish cutting, the depth-of-cut of each pass, the (variable) feed rate, and, in the case of five-axis machining, the lead and yaw angle of the tool, all of which affecting the power consumption and the tool wear. Additionally, unlike drilling, for general machining, the tool path itself is also a critical factor affecting the final total energy consumption. As an initial step, we will assume a fixed pattern of tool path (e.g., the iso-planar type) and also fixed lead and yaw angles of the tool, and establish the prediction models of the tool wear and power consumption as functions of the number of passes of semi-finish cutting, the depth-of-cut of each pass, and the feed rate.

Acknowledgements

This study is co-supported by the Major National Science and Technology Projects (No. 2017ZX04011430) and the Shanxi Provincial Key Research and Development Program (No. 2018ZDXM-GY-063).

References

Budak, E., Altintas, Y., Armarego, E.J.A., 1996. Prediction of milling force coefficients from orthogonal cutting data. *J. Manuf. Sci. Eng.* 118 (2), 216–224. <https://doi.org/10.1115/1.2831014>.

- Camposeco-Negrete, C., de Dios Calderón-Nájera, J., 2019. Sustainable machining as a mean of reducing the environmental impacts related to the energy consumption of the machine Tool : a case study of AISI 1045 steel machining. *Int. J. Adv. Manuf. Technol.* 102, 27–41. <https://doi.org/10.1007/s00170-018-3178-0>.
- Cuppini, D., D'errico, G., Rutelli, G., 1990. Tool wear monitoring based on cutting power measurement. *Wear* 139 (2), 303–311. [https://doi.org/10.1016/0043-1648\(90\)90052-C](https://doi.org/10.1016/0043-1648(90)90052-C).
- Fernández-Pérez, J., Cantero, J.L., Díaz-Álvarez, J., Miguélez, M.H., 2017. Influence of cutting parameters on tool wear and hole quality in composite aerospace components drilling. *Compos. Struct.* 178, 154–161. <https://doi.org/10.1016/j.compstruct.2017.06.043>.
- Gutowski, T.G., Branham, M.S., Dahmus, J.B., Jones, A.J., Thiriez, A., Sekulic, D.P., 2009. Thermodynamic analysis of resources used in manufacturing processes. *Environ. Sci. Technol.* 43 (5), 1584–1590. <https://doi.org/10.1021/es8016655>.
- Han, C., Zhang, D., Luo, M., Wu, B., 2018. Chip evacuation force modelling for deep hole drilling with twist drills. *Int. J. Adv. Manuf. Technol.* 3091–3103. <https://doi.org/10.1007/s00170-018-2488-6>.
- Hou, Y., Zhang, D., Wu, B., Luo, M., 2015. Milling force modeling of worn tool and tool flank wear recognition in end milling. *IEEE ASME Trans. Mechatron.* 20 (3), 1024–1035. <https://doi.org/10.1109/TMECH.2014.2363166>.
- Hu, S., Liu, F., He, Y., Peng, B., 2010. Characteristics of additional load losses of spindle system of machine tools. *J. Adv. Mech. Des. Syst. Manuf.* 4 (7), 1221–1233. <https://doi.org/10.1299/jamdsm.4.1221>.
- Hu, S., Liu, F., He, Y., Hu, T., 2012. An on-line approach for energy efficiency monitoring of machine tools. *J. Clean. Prod.* 27, 133–140. <https://doi.org/10.1016/j.jclepro.2012.01.013>.
- Iliescu, D., Gehin, D., Gutierrez, M.E., Girot, F., 2010. Modeling and tool wear in drilling of CFRP. *Int. J. Mach. Tool Manuf.* 50 (2), 204–213. <https://doi.org/10.1016/j.ijmachtools.2009.10.004>.
- Jia, S., Yuan, Q., Cai, W., Li, M., Li, Z., 2018. Energy modeling method of machine-operator system for sustainable machining. *Energy Convers. Manag.* 172, 265–276. <https://doi.org/10.1016/j.enconman.2018.07.030>.
- Kara, S., Li, W., 2011. Unit process energy consumption models for material removal processes. *CIRP Ann.* 37–40. <https://doi.org/10.1016/j.cirp.2011.03.018>.
- Lee, P., Altintas, Y., 1996. Prediction of ball-end milling forces from orthogonal cutting data. *Int. J. Mach. Tool Manuf.* 36 (9), 1059–1072. [https://doi.org/10.1016/0890-6955\(95\)00081-X](https://doi.org/10.1016/0890-6955(95)00081-X).
- Li, W., Kara, S., 2011. An empirical model for predicting energy consumption of manufacturing processes: a case of turning process. *Proc. IME B J. Eng. Manuf.* 225 (9), 1636–1646. <https://doi.org/10.1177/2041297511398541>.
- Li, L., Yan, J., Xing, Z., 2013. Energy requirements evaluation of milling machines based on thermal equilibrium and empirical modelling. *J. Clean. Prod.* 52, 113–121. <https://doi.org/10.1016/j.jclepro.2013.02.039>.
- Liu, N., Zhang, Y.F., Lu, W.F., 2015. A hybrid approach to energy consumption modelling based on cutting power: a milling case. *J. Clean. Prod.* 104, 264–272. <https://doi.org/10.1016/j.jclepro.2015.05.049>.
- Liu, Z.Y., Guo, Y.B., Sealy, M.P., Liu, Z.Q., 2016. Technology energy consumption and process sustainability of hard milling with tool wear progression. *J. Mater. Process. Technol.* 229, 305–312. <https://doi.org/10.1016/j.jmatprotec.2015.09.032>.
- Luo, M., Luo, H., Zhang, D., Tang, K., 2018. Improving tool life in multi-Axis milling of Ni-based superalloy with ball-end cutter based on the active cutting edge shift strategy. *J. Mater. Process. Technol.* 252, 105–115. <https://doi.org/10.1016/j.jmatprotec.2017.09.010>.
- Ma, F., Zhang, H., Cao, H., Hon, K.K.B., 2017. An energy consumption optimization strategy for CNC milling. *Int. J. Adv. Manuf. Technol.* 90 (5–8), 1715–1726. <https://doi.org/10.1007/s00170-016-9497-0>.
- Portillo, E., Cabanes, I., Sánchez, J.A., Orive, D., Ortega, N., Marcos, M., 2012. A computer assistant for monitoring tool performance during the drilling process. *Int. J. Comput. Integr. Manuf.* 25 (9), 829–838. <https://doi.org/10.1080/0951192X.2012.671540>.
- Proteau, A., Tahan, A., Thomas, M., 2019. Specific cutting energy: a physical measurement for representing tool wear. *Int. J. Adv. Manuf. Technol.* 1–10. <https://doi.org/10.1007/s00170-019-03533-4>.
- Shao, H., Wang, H.L., Zhao, X.M., 2004. A cutting power model for tool wear monitoring in milling. *Int. J. Mach. Tool Manuf.* 44 (14), 1503–1509. <https://doi.org/10.1016/j.ijmachtools.2004.05.003>.
- Shi, K.N., Zhang, D.H., Liu, N., Wang, S.B., Ren, J.X., Wang, S.L., 2018. A novel energy consumption model for milling process considering tool wear progression. *J. Clean. Prod.* 184, 152–159. <https://doi.org/10.1016/j.jclepro.2018.02.239>.
- Sun, Y., Sun, J., Li, J., Li, W., Feng, B., 2013. Modeling of cutting force under the tool flank wear effect in end milling Ti6Al4V with solid carbide tool. *Int. J. Adv. Manuf. Technol.* 69 (9–12), 2545–2553. <https://doi.org/10.1007/s00170-013-5228-y>.
- Sun, S., Brandt, M., Palanisamy, S., Dargusch, M.S., 2015. Effect of cryogenic compressed air on the evolution of cutting force and tool wear during machining of Ti–6Al–4V alloy. *J. Mater. Process. Technol.* 221, 243–254. <https://doi.org/10.1016/j.jmatprotec.2015.02.017>.
- Tian, C., Zhou, G., Zhang, J., Zhang, C., 2019. Optimization of cutting parameters considering tool wear conditions in low-carbon manufacturing environment. *J. Clean. Prod.* 226, 706–719. <https://doi.org/10.1016/j.jclepro.2019.04.113>.
- Wang, X., Williams, R.E., Sealy, M.P., Rao, P., Guo, Y., 2018. Stochastic modeling and analysis of spindle energy consumption during hard milling with a focus on tool wear. In: *ASME 2018 13th International Manufacturing Science and Engineering Conference*. American Society of Mechanical Engineers (pp. V003T02A002–

- V003T02A002). <https://doi.org/10.1115/MSEC2018-6511>.
- Wang, L., Meng, Y., Ji, W., Liu, X., 2019. Cutting energy consumption modelling for prismatic machining features. *Int. J. Adv. Manuf. Technol.* 1–11. <https://doi.org/10.1007/s00170-019-03667-5>.
- Watson, J.K., Taminger, K.M.B., 2018. A decision-support model for selecting additive manufacturing versus subtractive manufacturing based on energy consumption. *J. Clean. Prod.* 176, 1316–1322. <https://doi.org/10.1016/j.jclepro.2015.12.009>.
- Xu, K., Luo, M., Tang, K., 2016. Machine based energy-saving tool path generation for five-axis end milling of freeform surfaces. *J. Clean. Prod.* 139, 1207–1223. <https://doi.org/10.1016/j.jclepro.2016.08.140>.
- Yoon, H.S., Moon, J.S., Pham, M.Q., Lee, G.B., Ahn, S.H., 2013. Control of machining parameters for energy and cost savings in micro-scale drilling of PCBs. *J. Clean. Prod.* 54, 41–48. <https://doi.org/10.1016/j.jclepro.2013.04.028>.
- Yoon, H.S., Lee, J.Y., Kim, M.S., Ahn, S.H., 2014. Empirical power-consumption model for material removal in three-axis milling. *J. Clean. Prod.* 78, 54–62. <https://doi.org/10.1016/j.jclepro.2014.03.061>.
- Zeng, Y., Li, T., Deng, Y., Yuan, C., 2019. A general empirical energy consumption model for computer numerical control milling machine. *J. Manuf. Sci. Eng.* 141, 1–7. <https://doi.org/10.1115/1.4042306>.
- Zhao, J., Li, L., Wang, Y., Sutherland, J.W., 2019. Impact of surface machining complexity on energy consumption and efficiency in CNC milling. *Int. J. Adv. Manuf. Technol.* 1–15. <https://doi.org/10.1007/s00170-019-03334-9>.
- Zhong, Q., Tang, R., Peng, T., 2017. Decision rules for energy consumption minimization during material removal process in turning. *J. Clean. Prod.* 140, 1819–1827. <https://doi.org/10.1016/j.jclepro.2016.07.084>.